Welding in the World (2018) 62:1073–1081
https://doi.org/10.1007/s40194-018-0604-8

RESEARCH PAPER

Build-up strategies for temperature control using laser metal deposition for additive manufacturing

Torsten Petrat[1] · René Winterkorn[2] · Benjamin Graf[1] · Andrey Gumenyuk[1,2] · Michael Rethmeier[1,2]

Received: 2 August 2017 / Accepted: 8 May 2018 / Published online: 25 May 2018

Abstract

The track geometry created with laser metal deposition (LMD) is influenced by various parameters. In this case, the laser power has an influence on the width of the track because of an increasing energy input. A larger melt pool is caused by a rising temperature. In the case of a longer welding process, there is also a rise in temperature, resulting in a change of the track geometry. This paper deals with the temperature profiles of different zigzag strategies and spiral strategies for additive manufacturing. A two-color pyrometer is used for temperature measurement on the component surface near the melt pool. Thermocouples measure the temperatures in deeper regions of a component. The welds are located in the center and in the edge area on a test part to investigate the temperature evolution under different boundary conditions. The experiments are carried out on substrates made from mild steel 1.0038 and with the filler material 316L. The investigations show an influence on the temperature evolution by the travel path strategy as well as the position on the part. This shows the necessity for the development and selection of build-up strategies for different part geometries in additive manufacturing by LMD.

Keywords Laser welding · Temperature distribution · Laser surfacing · Clad steels · Heat flow

1 Introduction

Additive manufacturing technologies allow fast component manufacturing, which can save time and money by the development of new machines. Due to the tool-free production, new design freedom is also created. In order to take advantage of the potential, a rethinking of the design is necessary [1, 2]. Laser metal deposition (LMD) is already used in industrial applications for the repair and coating of components in the areas of toolmaking, turbine construction, and mechanical engineering, but is also increasingly used in the area of additive manufacturing of new parts [3–6]. This requires a more comprehensive knowledge of the process and its control [7]. The production of high-quality components can only be carried out by way of a complete process control, since a large number of additional factors must be considered for additive manufacturing. Therefore, current research projects investigate different areas in this field.

In the case of LMD, a laser beam melts a base material and powder as filler material, which is fed by a powder nozzle. After solidification of the material, a layer with metallurgical bonding without pores and cracks is formed. The process is characterized by a small weld pool, resulting in a low dilution of base material and filler material. Furthermore, the heat input and thus also the heat-affected zone are small and the cooling rate is high, resulting in a fine-grained structure [6]. The main parameters are laser power, powder feed rate, welding speed, and laser spot diameter. These allow prediction of the track geometry.

The laser power and the welding speed have a substantial influence on the track width, while the track height is mainly influenced by the powder feed rate and the welding speed [8].

The component is produced in layers, for which the component is sliced into individual layers. One layer can be built by different travel paths. In order to produce components which consist of many of these superimposed layers, an even surface is necessary. Irregularities add up over multiple layers and lead to error propagation and can influence the mechanical properties. In general, the overlap rates are between 30 and

This article is part of the collection Welding, Additive Manufacturing and Associated NDT

✉ Torsten Petrat
torsten.petrat@ipk.fraunhofer.de

[1] Fraunhofer Institute for Production Systems and Design Technology, Pascalstraße 8-9, 10587 Berlin, Germany

[2] Federal Institute for Materials Research and Testing, Unter den Eichen 87, 12205 Berlin, Germany

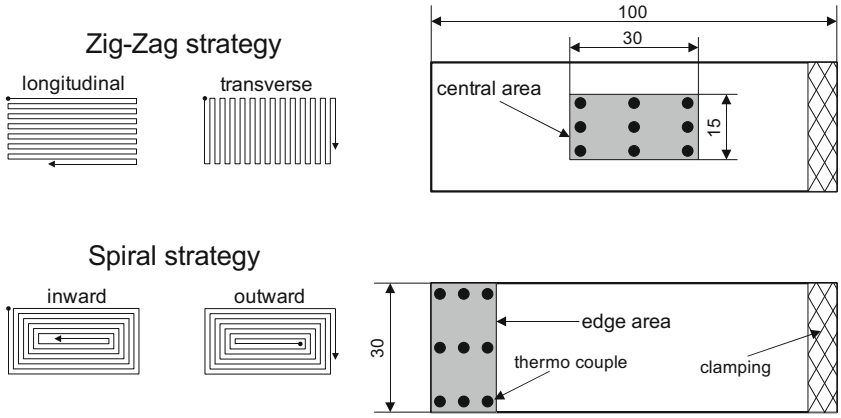

Fig. 1 Build-up strategies for individual layers in different areas

50% [9, 10]. Zigzag and spiral strategies are typical and are often supported by a contour tool path for higher volumes [11–13]. Software packages for tool path planning are already available on the market but are constantly being further developed, because consistent predictions of the material build-up are not reliable yet, due to the different environmental influences during the manufacturing process [14]. The adaptation of build-up strategies makes it possible to influence the layer structure and predict constant manufacturing sequences [11, 15]. At the same time, the build-up strategies have an influence on the welding distortion and the residual stresses [16]. These interactions must be taken into account by the design of layer strategies in order to be able to derive an optimal compromise.

The yield strength and ultimate tensile strength of components manufactured by LMD have similar or higher values than forged components. A heat treatment after the production is often necessary to optimize the elongation properties [17]. The thermal history influences further mechanical properties like hardness. Farshidianfar et al. showed a significant correlation between cooling rate and grain size [18]. A fine-grained microstructure could be found with high cooling rates, while coarse microstructure was detected with a decrease in cooling rate. Investigations also show that the mechanical properties differ depending on the direction of stress. Guo et al. examined that the tensile strength, yield strength, and elongation at stress parallel to the layer are higher than parallel to the build-up direction [19]. A segregation of alloy elements may occur depending on parameters. Zhong et al. showed this for the powder bed process selective laser melting [20]. Similar investigations with LMD already exist for nickel-base alloys. Segregation can result in phases with undesired properties, e.g., embrittlement [21, 22]. For this reason, it is necessary to prevent this separation to achieve optimum properties by selecting correct parameters.

During the manufacturing process of 3D components, the boundary conditions vary due to changing geometries and thermal effects. This can lead to overheating, resulting in defects such as pores or evaporation of alloying elements, which adversely affect the density as well as the alloy composition [23]. A further point is the changes in the track geometry, which make a prediction of the material deposition more difficult. This problem has to be solved in order to enable process automation and thus an application in the industrial serial production. In order to ensure constant temperatures and an even build-up, close-loop control systems have already been developed. Two variants are used to achieve a constant weld pool temperature by adjusting the laser power. A variant uses an image evaluation of the recorded weld pool and adjusts the process according to the measured pool size [24]. In a further variant, two-color pyrometers are used to determine the temperature in the weld pool [25, 26]. A proactive control of the expected effects reduces the necessary intervention by the control algorithms, e.g., during process start as well as by reaching edges. This knowledge of the use of adapted build-up strategies leads to a continuous process with improved results.

The different investigations show that extensive knowledge about the process behavior is necessary in order to be able to choose optimal build-up strategies. This improves the possible prediction of the properties and quality of components produced by LMD.

2 Experimental

In the experiments, different build-up strategies are tested, which are used in additive manufacturing with LMD. To examine the temperature behavior under different boundary conditions transverse and longitudinal zigzag strategies as well as inward and outward directed spiral strategies are studied, which are shown in Fig. 1. The dimension of the clad area is 15×30 mm^2. To gain a track width of 2 mm, the following

Table 1 Chemical composition of Metco™ 41C

Product name	Weight in %								
	Fe	C	Cr	Mn	Mo	Ni	P	S	Si
Metco 41C	Bal.	0.02	17.3	0.12	2.3	11.9	0.00	0.01	2.5

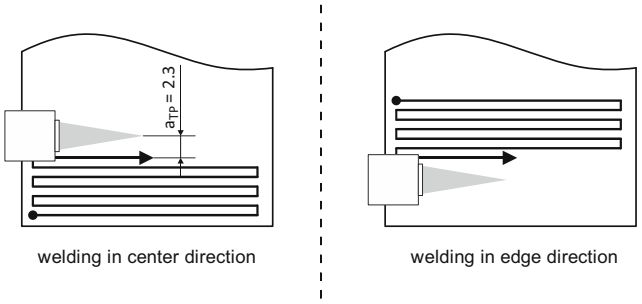

Fig. 2 Offset directions of zigzag strategies

parameter set is used: laser power $P_L = 800$ W, welding velocity $v = 600$ mm/min, spot diameter $d = 1.2$ mm, and powder mass flow $m_P = 4.4$ g/min.

The longitudinal zigzag strategy consists of 14 single tracks with an overlap of 1 mm and a length of 30 mm. The transverse zigzag strategy comprises of 29 tracks with a length of 15 mm. Spiral strategies consist of longitudinal and transverse tracks with changing lengths. The first track of the inward directed spiral is a 15-mm-long transverse track. It is followed by a longitudinal track of 30-mm length. The next transverse track is 1 mm shorter than the previous transverse track. The same applies to the longitudinal tracks. All following transverse and longitudinal tracks are 2 mm shorter than the previous track. The central, longitudinal track is 15 mm long. The outward directed spiral is manufactured in the reverse order.

The substrate material is mild steel 1.0038 with a thickness of 6 mm. The strategies are welded on the central area (A_C) as well as on the edge area (A_E) of the test piece, in order to investigate influences on the temperature by using build-up strategies at different boundary conditions. The dimensions of the test piece and the position of the areas A_C and A_E are shown on the right side of Fig. 1.

The powder Metco™ 41C is used as a filler material and corresponds to 316L (stainless steel). The exact chemical composition is shown in Table 1.

Thermocouples (TC) are used to measure the temperature. Nine thermocouples of type K are attached on the bottom of the test piece. In addition, a two-color pyrometer records the surface temperature near the weld pool while welding the zigzag strategies. The measuring range of the pyrometer Metis MQ22 extends from 350 to 1300 °C. A distance of $a_{TP} = 2.3$ mm lies between laser spot and pyrometer spot to detect the substrate temperature and to minimize the disruption by the weld pool. A spot position parallel to the track allows a measurement independent of direction. The distance a_{TP} is indicated in Fig. 2. The measuring spot of the pyrometer is always adjusted as shown in Fig. 2 and measures on the test piece itself. Furthermore, the influence of the welding direction for zigzag strategies in center direction (Fig. 2, left) and in edge direction (Fig. 2, right) are examined.

3 Results and discussion

3.1 The influence of pre and post manufactured tracks on the maximum temperatures of zigzag strategies

For the analysis of the different build-up strategies, the maximum temperatures of the various TCs are used. The thermocouples can be grouped for the zigzag strategies, whereby the three TCs on one tracks form a group. The groups are reached chronologically in the course of the zigzag strategy from start to end position. Figure 3 shows the temperature courses of the middle TCs of the transverse zigzag strategy in the central area. The middle TCs reach the highest temperature values of a group. It must be acknowledged, that the maximum TC temperature is not strictly connected to the passing time of the weld pool on the upper surface. The start of welding (SOW) corresponds to 6 s.

Group 1 is located right under the first track of the transverse zigzag strategy (Fig. 3b), while the maximum temperatures of this group are reached at 56.5 s, which is after the

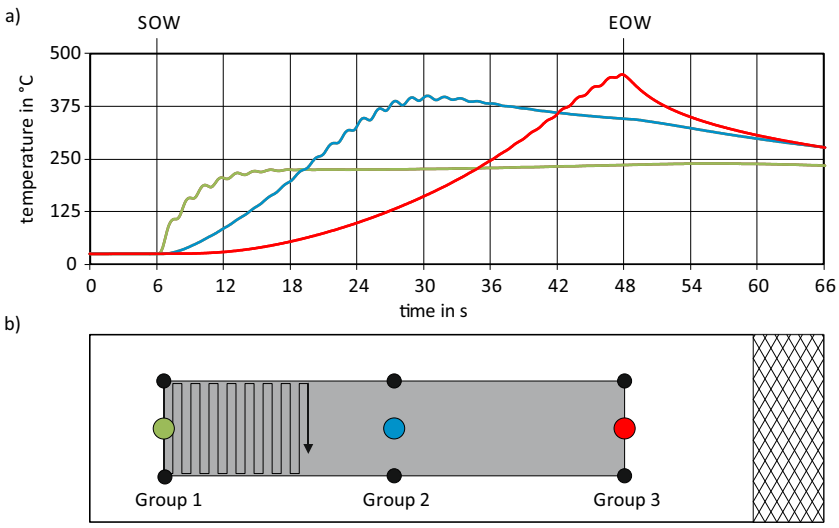

Fig. 3 Transverse zigzag strategy in the central area. **a** Temperature of the thermocouples. **b** Color code and arrangement of TC

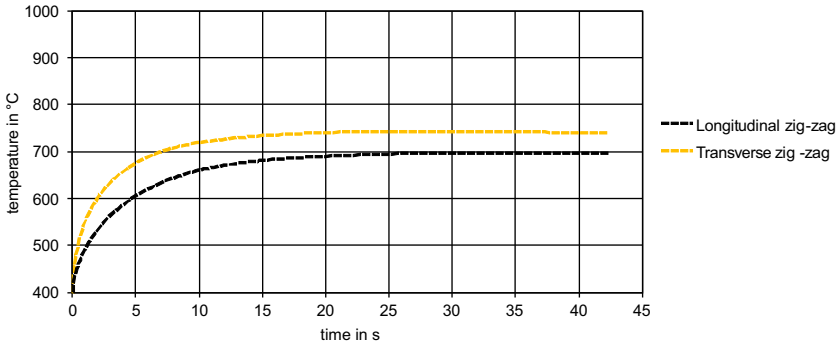

Fig. 4 Temperature profile of zigzag strategies in the central area

welding process. This is due to the fact that the temperature of the whole substrate is 25 °C at the start of the welding. The heat spreads to all sides with a high cooling rate. In the first 6 s, a fast temperature rise of TC group 1 can be seen. After a time of 16 s, the TC reaches 225 °C and remains nearly constant with a small and linear increase till the end of the welding (EOW). The curve shows a continuous increase of temperature of group 2 right from the start and at the time of 13 s the temperatures are exceeding those of group 1. This is due to the fact that the whole test piece is accumulating the heat of the welding process. When the laser reaches the surface of group 2, the temperature is at 375 °C. As in the first group, the maximum temperature does not occur, while the weld pool is located directly above the TC. This can be attributed to the delay due to the heat conduction. For this reason, the middle TC of group 2 reaches its maximum of 400 °C at 24.4 s, which corresponds with the manufacturing of the 17th track. In contrast to group 1, the temperatures of the group 2 fall after reaching their maximum value. Group 3 is located under the last weld track of the transverse zigzag strategy (Fig. 3b) and has the longest preheating time. This results in the highest temperatures. The zigzag strategy process ends right above the last TCs and the maximum temperature are occurring with the last track. The energy input stops with the EOW and the substrate does not heat up any longer.

3.2 Central area

Figure 4 shows temperature graphs of the zigzag strategies in the central area, which are recorded with the pyrometer. Both zigzag strategies resemble an asymptotic course. In the first 5 s, a rapid increase in temperature is measured. In the continuing process, the temperature rises slowly to a maximum of 700 °C for the longitudinal zigzag strategy and a maximum of 740 °C for the transverse zigzag strategy. The stronger temperature increase of the transverse zigzag strategy can be attributed to the shorter direction changes compared to the longitudinal zigzag strategy.

Longitudinal zigzag strategy Figure 5 illustrates the heat dissipation (a), the heat tint (b), and the maximum temperatures (c) for the longitudinal zigzag strategy in the central area ($ZZ_{long,\ cent}$) measured by the thermocouples. The bars of this chart have to be seen in groups, which are reached successively in the course of the measurement. The bar chart shows that the maximum temperatures of the groups are gradually increasing. The increase of the middle TCs (5 and 8) is higher than that of the outer ones.

The temperatures of group 1 - TC 1-2-3 are between 263.59 and 318.69 °C. TC 2 shows the highest temperature. One reason is the number of welding. TC 2 is reached twice as often as TC 1 and 3, which lead to a higher heat input. The surrounding material of the outer thermocouples is colder at the start with the result of higher heat dissipation, which is illustrated with red lines in Fig. 5. This fact applies also for TC 5 and 8. Due to the preheating that is described earlier, the temperature gradient between weld track and substrate of group 2 - TC 4-5-6 is generally smaller. This results in higher maximum temperatures than those of group 1 - TC 1-2-3. They are between 304.87 and 387.01 °C. TC 4 and 6 mostly dissipate their heat to one side and downwards while TC 5

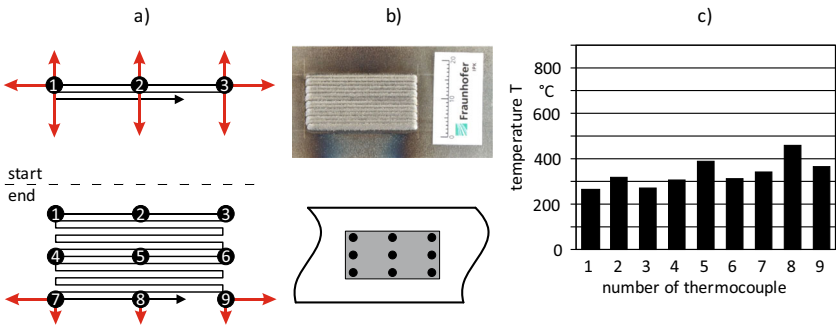

Fig. 5 Longitudinal zigzag, central area. **a** Change of heat dissipation in process. **b** Position of cladding on substrate. **c** Bar chart of maximum temperatures

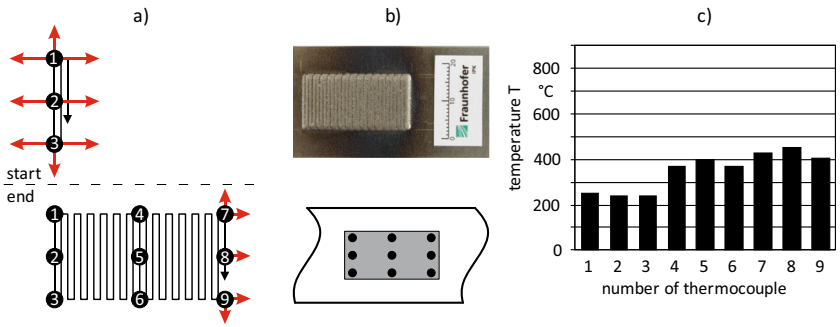

Fig. 6 Transverse zigzag, central area. **a** Change of heat dissipation in process. **b** Position of cladding on substrate. **c** Bar chart of maximum temperatures

primary dissipates downwards (Fig. 5a, middle). Group 3 - TC 7-8-9 behaves similar. Because of the preheating and heat accumulation at the edge of the test piece, the highest temperatures are reached in this group. The lowest temperature of the third group is about 338.49 °C, which is higher than the maximum of group 1 - TC 1-2-3. The highest temperature of group 3 - TC 7-8-9 occurs at TC 8 and is also the absolute maximum of $ZZ_{long,\ cent}$. It shows 456.35 °C. The heat accumulation at the edge leads to the smallest temperature gradient. The heating around TC 8 can be seen in the heat tint in Fig. 5b. The difference between the lowest maximum (TC 1) and the absolute maximum (TC 8) is 192.76 °C.

Transverse zigzag strategy The thermocouples of the transverse zigzag strategy in the central area $ZZ_{trans,\ cent}$ can also be divided in three groups. The bar chart in Fig. 6c shows that the maximum temperatures of $ZZ_{trans,\ cent}$ are raising gradually. Group 1 - TC 1-2-3 lies on the left side and is located right under the first track. The temperature of the whole substrate is around 25 °C. This leads to the highest temperature gradients between weld track and substrate by process start. This context is illustrated in Fig. 6a, left. The main dissipation directions are positive and negative to the offset direction. Group 1 - TC 1-2-3 is consequently reaching the lowest maximum temperatures. They are between 237.99 and 248.27 °C. Group 2 - TC 4-5-6 is passed after the half welding time. The lowered temperature gradients (Fig. 6, middle) and the so far accumulated heat lead to higher temperatures. The middle thermocouple shows the highest temperature of this group with 400.03 °C. The maxima of group 1 - TC 1-2-3 and group 2 - TC 4-5-6 differ by 151.76 °C. The maximum temperatures of group 3 - TC 7-8-9 are the highest. This includes that group 3 - TC 7-8-9 has the minimum temperature gradients and thereby even lower heat dissipation than group 2 - TC 4-5-6. TC 8 shows 450.70 °C, which is the absolute maximum temperature of $ZZ_{trans,\ cent}$. The strongest heat tint is located between groups 2 and 3 (Fig. 6b). This means that this area is under the biggest thermal influence. This reflects the observation that the difference between group 2 - TC 4-5-6 and group 3 - TC 7-8-9 is much lower than that between group 1 - TC 1-2-3 and group 2 - TC 4-5-6. The maximum temperature difference in $ZZ_{trans,\ cent}$ occurs between TC 3 and TC 8 and amounts 212.71 °C.

Inward directed spiral The TC of the inward directed spiral in the central area ($S_{in,\ cent}$) can be categorized by the distance to the center of the spiral (COS). Group 1 - TC 1-3-7-9 has the largest distance to the center point and is located in the corners of the spiral. The next nearest distance shows group 2 - TC 4-6. TC 4 and TC 6 are attached to the middle of the transverse side. TC 2 and TC 8 are located at the middle of the longitudinal sides and represent group 3 - TC 2-8. Group 4 - TC 5 consists of TC 5 that lies in the COS. The bar chart in Fig. 7c shows the maximum temperatures that were reached during the welding. The charts are arranged according to the distance to the COS.

Group 1 - TC 1-3-7-9 and group 2 - TC 4-6 have the longest cooling times, before the welding passes this region again. This leads to high heat dissipation and low maximum temperatures of about 300 °C. Group 1 - TC 1-3-7-9 shows

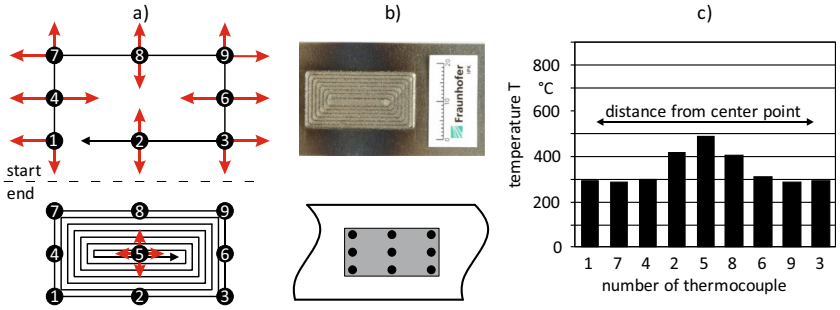

Fig. 7 Inward directed spiral, central area. **a** Change of heat dissipation in process. **b** Position of cladding on substrate. **c** Bar chart of maximum temperatures

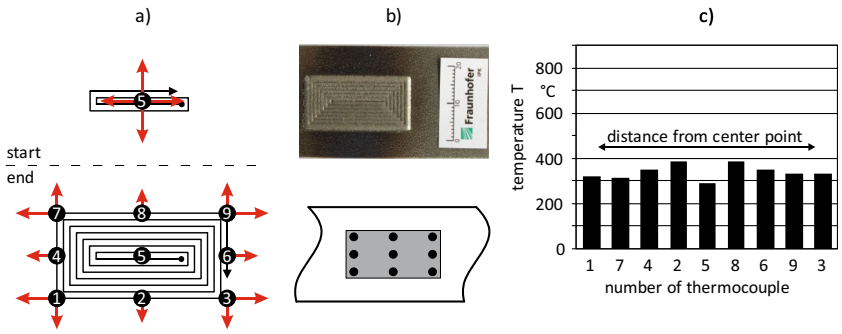

Fig. 8 Outward directed spiral, central area. **a** Change of heat dissipation in process. **b** Position of cladding on substrate. **c** Bar chart of maximum temperatures

maximum temperatures between 287.70 and 293.00 °C. Group 2 - TC 4-6 lies slightly nearer to the COS and shows also slightly higher maximum temperatures. TC 4 reaches 300.86 °C and TC 6 shows a maximum of 310.24 °C. The heat dissipation of group 3 - TC 2-8 is lower. This is due to the close proximity to the edge of the test piece. The maximum temperature of group 3 - TC 2-8 is 416.78 °C. The maximum of group 4 - TC 5 is 488.49 °C, which is the absolute maximum of $S_{in,\ cent}$. The tool path results in a heat accumulation, because of the preheated material. The influenced heat gradients are illustrated at the left part of Fig. 7a (end). The difference between the highest and lowest maximum temperature in the inward directed spiral is 200.78 °C.

Outward directed spiral The TC of the outward directed spiral in the central area ($S_{out,\ cent}$) are also organized by the distance to the COS. This leads to the following groups: group 1 - TC 5, group 2 - TC 2-8, group 3 - TC 4-6, and group 4 - TC 1-3-7-9. Group 1 - TC 5 lies in the center of the outward directed spiral. Figure 8 (begin) shows the first tracks of the outward directed spiral. High heat gradients caused of cold substrate allows a high heat dissipation to all directions. TC 5 is not passed again and shows the lowest temperature of 294.70 °C.

Table 2 shows the differences of the minimum and maximum temperature for the strategies in the central area. The maximum values of the TCs do not show the 40 °C difference of the transverse compared to the longitudinal strategy, which is seen in the pyrometer measurements in Fig. 4. The temperature effect is converse with a higher maximum temperature of the longitudinal strategy. It looks like, that the thermal history of regions with higher distance to the melt pool is influenced by the welding strategy.

In comparison of all strategies, $S_{out,\ cent}$ has the smallest maximum temperature with 387.96 °C as well as the smallest temperature differences with 93.26 °C (24%). This means that $S_{out,\ cent}$ has the lowest thermal influences on lower substrate regions and the most uniform heat distribution. Therefore, it is advisable to use outward spirals in central manufacturing areas.

3.3 Edge area

Zigzag strategies The zigzag strategies are considered in the following. The longitudinal zigzag strategy with offset in center direction $ZZ_{long,\ cd}$, the longitudinal zigzag strategy with offset in edge direction $ZZ_{long,\ ed}$ and the transverse zigzag strategy $ZZ_{trans,\ edge}$ (see Fig. 2 to differentiate $ZZ_{long,\ cd}$ and $ZZ_{long,\ ed}$). The temperature profile recorded by means of a pyrometer is shown in Fig. 9. A different course in the curves of the individual strategies is recognizable. $ZZ_{long,\ cd}$ has an asymptotic course similar to the zigzag strategies in the center area. $ZZ_{long,\ ed}$ and $ZZ_{trans,\ edge}$ show a temperature rise followed by a constant course and a renewed increase at the component edge. Heat accumulation occurs in the edge area, since the heat input cannot be dissipated to surrounding material. This increases the temperature at the end of the welding process.

Figure 10 shows the maximum temperatures of the zigzag strategies in the edge area. The evaluation of the thermocouple measurement reveals clear differences in the maximum temperatures among the longitudinal zigzag strategies as well as in comparison with $ZZ_{trans,\ edge}$.

The maximum temperatures of $ZZ_{long,\ cd}$ are illustrated on the left side of Fig. 10. The values are almost identical and lie

Table 2 Thermal values of strategies in the central area

Strategy	Maximum temperature in °C	Temperature difference in °C	Temperature difference in %	Figure
$ZZ_{long,\ cent}$	456.35	192.76	42	Fig. 5
$ZZ_{trans,\ cent}$	450.70	212.71	47	Fig. 6
$S_{in,\ cent}$	488.49	200.78	41	Fig. 7
$S_{out,\ cent}$	387.96	93.26	24	Fig. 8

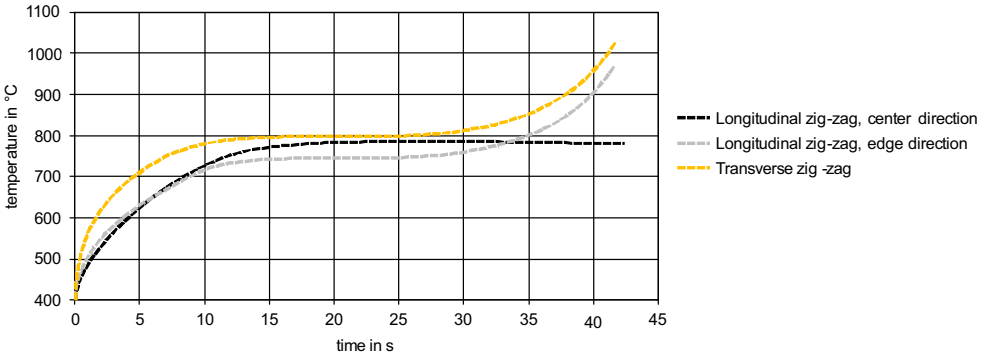

Fig. 9 Temperature profile of zigzag strategies in the edge area

between 509.41 to 549.19 °C, which leads to a maximum temperature difference of 39.78 °C.

Big temperature changes can be seen in both $ZZ_{trans,\ edge}$ and $ZZ_{long,\ ed}$. The temperatures increase steadily in the course of the welding process, and each thermocouple group reaches higher values than the preceding one.

A comparison of $ZZ_{long,\ cd}$ and $ZZ_{long,\ ed}$ shows that the maximum temperature of the first thermocouple group of $ZZ_{long,\ ed}$ is lower than the first thermocouple group of $ZZ_{long,\ cd}$. Thus, the maximum temperature of group 1 - TC 1-2-3 of $ZZ_{long,\ ed}$ is 441.10 °C and that of $ZZ_{long,\ cd}$ is 512.71 °C. This is due to heat dissipation in the particular areas. With $ZZ_{long,\ ed}$, the applied heat can be dissipated into the still cold component during the process start in both positive and negative welding direction. The process start at the component edge in strategy $ZZ_{long,\ cd}$ allows only heat dissipation in one direction and thus leads to a faster increase in component temperature.

A step change in temperature by 122.61 °C to a maximum of 573.62 °C is recognizable in group 2 - TC 4-5-6 of strategy $ZZ_{long,\ edge,\ ed}$; this is already above the maximum values of the strategy $ZZ_{long,\ cd}$. The influence of the heat in the direction of the component edge is already visible at half of the process time, which is reflected in a rising temperature. With a further increase of 126.30 °C in the last group of $ZZ_{long,\ ed}$, a maximum temperature of 699.92 °C is reached. The middle diagram of Fig. 10 shows a nearly identical temperature within a group. The temperatures of group 1 - TC 1-2-3 lie within 436.35 and 441.10 °C. Group 2 - TC 4-5-6 extends from 567.96 to 573.62 °C and group 3 - TC 7-8-9 from 697.73 to 699.92 °C. This is due to the influence of the given heat transfer. The heat accumulates in the peripheral areas of the external thermocouples, while the middle thermocouples are more frequently passed, but the heat can be dissipated in different directions. These result in uniform temperature values.

Step changes in temperature of the transverse zigzag strategy $ZZ_{trans,\ edge}$ can be seen in the right diagram of Fig. 10. These effects occur in the welding direction as well as within a thermocouple group. Due to the heat accumulation effects, the welding direction leads to an increase, as can be seen for strategy $ZZ_{long,\ ed}$. The level effects within a group come from the different conditions during the heat transfer. The closer the thermocouples are to the component

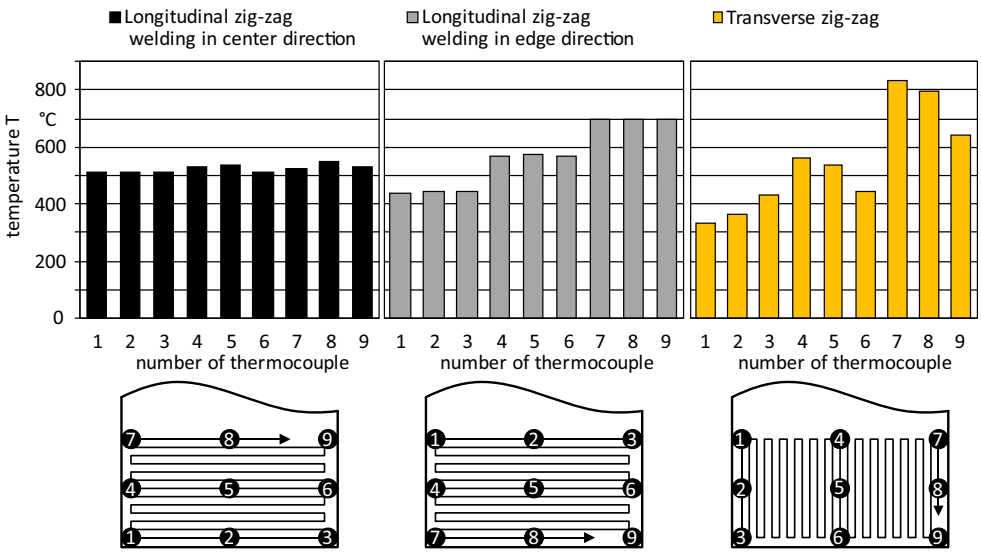

Fig. 10 Maximum temperatures of zigzag strategies in the edge area

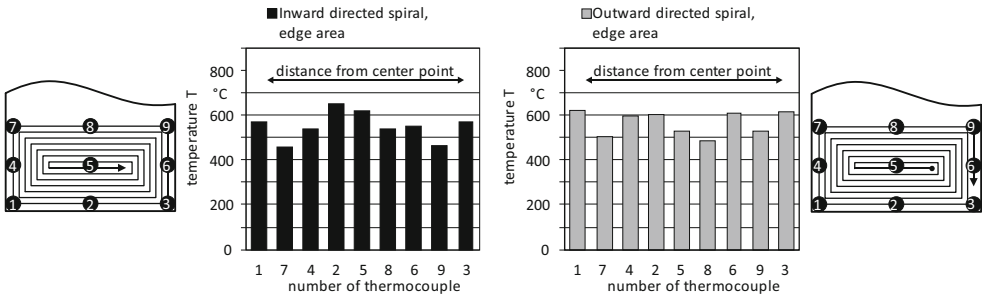

Fig. 11 Maximum temperatures of spiral strategies in the edge area

edge, the stronger the heat accumulation and the corresponding maximum temperature. Only in group 1 - TC 1-2-3 of $ZZ_{trans,\ edge}$ is another behavior recognizable, which is attributed to the low temperature of the component during the process start and the starting direction away from the component edge. The strongest heat build-up occurs in the corner area of the last welding track. TC 7 measures a maximum temperature of 833.67 °C, which is the highest temperature of all the tested layer strategies.

Spiral strategies Figure 11 illustrates the maximum temperatures of the spiral strategies in the edge area as well as the arrangement of the TC and the spiral strategies on the test piece. The bar chart of the inward directed spiral at the edge area $S_{in,\ edge}$ shows high differences in temperature within thermocouples of same distance. The position has a high influence, which can be seen by comparing TC 1 and TC 3 with TC 7 and TC 9. The thermocouples have the same distance, while the ones at the edge measure 20% higher temperatures. This is because the heat dissipation in the corners of the test piece is reduced. TC 4 and TC 6 with similar conditions show also similar maximum temperatures. TC 5 in the end position of the strategy measures a lower temperature as the near TC 2 at the edge of the component with the maximum temperature of 648.09 °C. TC 8 with the same the distance as TC 2 from the center point has a significant lower temperature. The lessened heat dissipation at the edge causes a movement of the temperature maxima in edge direction. The bars of TC 2, 5, and 8 show the rising temperature maxima in edge direction. The difference between minimum temperature of TC 7 with 456.18 °C and maximum temperature of TC 2 with 648.09 °C is 191.91 °C or 33%.

The bar chart of strategy $S_{out,\ edge}$ shows two different temperature levels, Fig. 11. TC 1, 2, 3, 4, and 6 vary between 603.09 and 623.08 °C, while TC 5, 7, 8, and 9 have temperatures from 491.06 to 531.55 °C. TC 5 is in the start area, which implies high heat dissipation. The following cladding process leads to heat accumulation in edge areas. The thermocouples within tool path and edge are showing the highest temperatures. TC 7 to 9 can dissipate the heat input to the colder substrate and measure smaller values. $S_{out,\ edge}$ has a difference of 132.02 °C (21%) between minimum and maximum temperature.

The differences of minimum temperatures and maximum temperature for the strategies of the edge area are listed in Table 3. The consideration of the zigzag strategies shows, that the temperature behavior of the pyrometer measurement, Fig. 9, can also be seen in the thermocouple measurements. A strong temperature increase next to the melt pool at the end results also in a high value at the bottom of the test piece. The heat accumulation can be identify at the top and allows a conclusion of the temperature behavior at the surface.

The maximum temperature of strategy $ZZ_{long,\ cd}$ is 34% lower than the maximum temperature of strategy $ZZ_{trans,\ edge}$ and shows the smallest difference of minimum and maximum with 39.78 °C (7%). Strategy $ZZ_{trans,\ edge}$, on the other hand, has a temperature difference of 59% within the strategy. For a low temperature influence at deeper regions of a test piece, the strategy $ZZ_{long,\ cd}$ should be used. The results show the high influence of a correct strategy choice for influencing the temperature development.

Table 3 Thermal values of strategies in the edge area

Strategy	Maximum temperature in °C	Temperature difference in °C	Temperature difference in %	Figure
$ZZ_{long,\ cd}$	549.19	39.78	7	Fig. 10
$ZZ_{long,\ ed}$	699.92	263,57	38	Fig. 10
$ZZ_{trans,\ edge}$	833.67	493,58	59	Fig. 10
$S_{in,\ edge}$	648.09	191.91	30	Fig. 11
$S_{out,\ edge}$	623.08	132.02	21	Fig. 11

4 Conclusion

The influence of different build-up strategies on the resulting maximum temperatures were investigated in this work. Studies on different zigzag and spiral strategies were carried out in a central area as well as in an edge area. Temperature measurements were made on the underside of a 6-mm-thick work piece by means of thermocouples in order to detect the influence in lower component areas. Differences between the individual strategies were shown. When using the same strategy in a different workpiece area, different temperature profiles occur.

Strong differences between the spiral strategies were detected in the central area of the workpiece. While the outward spiral strategy $S_{out,\ cent}$ shows the lowest maximum temperature of 388 °C as well as the smallest temperature difference of 93 °C between the thermocouples, the inward directed spiral strategy $S_{in,\ cent}$ increases the maximum temperature by 100 °C and a temperature difference by more than 200 °C.

All strategies showed increased peak temperatures in the edge area compared to the central area. A reduced heat transfer at the edges leads to heat accumulation and results in the detected temperature differences. A comparison of the zigzag strategies makes it clear, that the welding direction has a strong influence on the maximum temperatures. A longitudinal zigzag strategy in center direction reduces the maximum temperature around 150 °C compared to a weld in edge direction. The zigzag strategy $ZZ_{long,\ cd}$ shows the smallest maximum temperatures as well as the smallest temperature differences in the edge area.

It is found that adapted build-up strategies are necessary to ensure low maximum temperatures and low temperature differences under different boundary conditions.

Acknowledgments The authors would like to acknowledge the Federal Ministry of Education and Research (BMBF) for funding the research by their support program Wachstumskern Potenzial and the Federal Institute for Materials Research and Testing for support.

References

1. Graf B, M Schuch, R Kersting, A Gumenyuk (2015) Additive process chain using selective laser melting and laser metal deposition. Lasers Manuf Conf 2015
2. Vayre B, Vignat F, Villeneuve F (2012) Designing for additive manufacturing. Proc CIRP 3:632–637
3. DMG MORI, Hoedtke GmbH & Co. KG - Generative Komplettbearbeitung in Fertigteilqualität". [Online]. Verfügbar unter: http://de.dmgmori.com/fachpresse/advanced-technologies/hoedtke-gmbh—co–kg—generative-komplettbearbeitung-in-fertigteilqualitaet/385532
4. DMG MORI, Additive manufacturing eröffnet neue Designmöglichkeiten in der Herstellung von 3D-Bauteilen. [Online]. Verfügbar unter: http://de.dmgmori.com/fachpresse/advanced-technologies/additive-manufacturing/441798
5. Graf B, Gumenyuk A, Rethmeier M (2012) Laser metal deposition as repair technology for stainless steel and titanium alloys. Phys Proc 39:376–381
6. Kaierle S, Barroi A, Noelke C, Hermsdorf J, Overmeyer L, Haferkamp H (2012) Review on laser deposition welding: from micro to macro. Phys Proc 39:336–345
7. Khazan P, Stroth M, Freiße H, Köhler H (2014) Mechanical properties of large three-dimensional specimens build through direct powder deposition. Adv Mater Res 1018:525–532
8. Graf B, Ammer S, Gumenyuk A, Rethmeier M (2013) Design of experiments for laser metal deposition in maintenance, repair and overhaul applications. Proc CIRP 11:245–248
9. Cao Y, Zhu S, Liang X, Wang W (2011) Overlapping model of beads and curve fitting of bead section for rapid manufacturing by robotic MAG welding process. Robot Comput Integr Manuf 27(3):641–645
10. Li Y, Ma J (1997) Study on overlapping in the laser cladding process. Surf Coat Technol 90:1–5
11. Petrat T, Graf B, Gumenyuk A, Rethmeier M (2015) Build-up strategies for generating components of cylindrical shape with laser metal deposition. Lasers Manuf Conf 2015
12. Rombouts M, Maes G, Hendrix W, Delarbre E, Motmans F (2013) Surface finish after laser metal deposition. Phys Proc 41:803–807
13. Tabernero I, Lamikiz A, Martínez S, Ukar E, Figueras J (2011) Evaluation of the mechanical properties of Inconel 718 components built by laser cladding. Int J Mach Tools Manuf 51(6):465–470
14. Siemens Industry Software GmbH, NX Hybrid additive manufacturing—the new art of manufacturing—going beyond 3D printing. [Online]. Verfügbar unter: https://www.plm.automation.siemens.com/de_de/products/nx/for-manufacturing/cam/hybrid-additive-manufacturing.shtml
15. Petrat T, Graf B, Gumenyuk A, Rethmeier M (2016) Laser metal deposition as repair technology for a gas turbine burner made of inconel 718. Phys Proc 83:761–768
16. Foroozmehr E, Kovacevic R (2010) Effect of path planning on the laser powder deposition process : thermal and structural evaluation. Int J Adv Manuf Technol 51:659–669
17. Yadollahi A, Shamsaei N, Thompson SM, Seely DW (2015) Effects of process time interval and heat treatment on the mechanical and microstructural properties of direct laser deposited 316L stainless steel. Mater Sci Eng A 644:171–183
18. Farshidianfar MH, Khajepour A, Gerlich AP (2016) Effect of real-time cooling rate on microstructure in laser additive manufacturing. J Mater Process Technol 231:468–478
19. Guo P, Zou B, Huang C, Gao H (2017) Study on microstructure, mechanical properties and machinability of efficiently additive manufactured AISI 316L stainless steel by high-power direct laser deposition. J Mater Process Technol 240:12–22
20. Zhong Y, Liu L, Wikman S, Cui D, Shen Z (2016) Intragranular cellular segregation network structure strengthening 316L stainless steel prepared by selective laser melting. J Nucl Mater 470:170–178
21. Cao J, Liu F, Lin X, Huang C, Chen J, Huang W (2013) Effect of overlap rate on recrystallization behaviors of laser solid formed Inconel 718 superalloy. Opt Laser Technol 45:228–235
22. Zhao X, Chen J, Lin X, Huang W (2008) Study on microstructure and mechanical properties of laser rapid forming Inconel 718. Mater Sci Eng A 478(1–2):119–124
23. Flynn JM, Shokrani A, Newman ST, Dhokia V (2016) Hybrid additive and subtractive machine tools—research and industrial developments. Int J Mach Tools Manuf 101:79–101
24. Wank A u. a. Closed-loop control tools for automated laser cladding processes
25. Bi G, Gasser A (2011) Restoration of nickel-base turbine blade knife-edges with controlled laser aided additive manufacturing. Phys Proc 12(1):402–409
26. Song L, Mazumder J (2011) Feedback control of melt pool temperature during laser cladding process. IEEE Trans Control Syst Technol 19(6):1349–1356